High Temperature Plastic-Flow Behavior of Mixtures of Austenite, Cementite, Ferrite, and Pearlite in Plain-Carbon Steels

P. J. WRAY

The plastic-flow behavior of ferrite + pearlite, pearlite + cementite, and austenite + cementite mixtures in plain carbon steels has been examined over the temperature range 500 to 1050 °C, strain-rate range 6×10^{-6} to 2×10^{-2} s^{-1}, and carbon range 0.005C to 1.89C. Up to the eutectoid temperature the strength of the ferrite + pearlite mixture more than doubles as the carbon content increases from 0.005C to 0.7C, so that whereas in low-carbon steels the ferrite is weaker than the higher temperature austenite phase, in eutectoid steels the fully pearlitic structure is stronger than the fully austenitic structure. Manganese and silicon strengthen ferrite more effectively than they do austenite. A 0.17 pct phosphorus addition strengthens the ferrite + pearlite mixture across the range of microstructures from fully ferritic to fully pearlitic. Beyond the eutectoid composition, the amount of proeutectoid cementite does not significantly affect the strength of the pearlite, but above the eutectoid temperature it appreciably strengthens the austenite and cementite mixture at the strain rate of 2×10^{-2} s^{-1}.

I. INTRODUCTION

To properly control high-temperature processes such as casting, welding, and thermomechanical treating, it is necessary to have a detailed knowledge of the plastic flow behavior of metals at elevated temperatures. In the case of steels, a number of phases and phase mixtures exist at elevated temperatures, as shown schematically in Figure 1, and each phase has its own characteristic deformation behavior. The most extensive phase is fcc austenite, and a considerable amount of information regarding its plastic flow behavior is now available.[1-4] Immediately below the austenite phase field but still above the eutectoid temperature are the two-phase mixtures of ferrite + austenite and austenite + cementite. The mechanical behavior in the ferrite + austenite region was recently examined in detail.[5] As for the mechanical behavior of the austenite + cementite mixture, most attention has been paid recently to the superplastic flow obtained when an ultrafine microstructure is produced by working in this two-phase region,[6,7,8] and there has been little interest in the deformation behavior of simply annealed austenite + cementite structures. Below the eutectoid temperature there are two mixtures — ferrite + pearlite in hypoeutectoid steels and pearlite + cementite in hypereutectoid steels. The variation of the plastic-flow behavior of these mixtures with carbon content at 600 °C is illustrated in Figure 2, and some related microstructures are shown in Figure 3. A major purpose of the present paper is

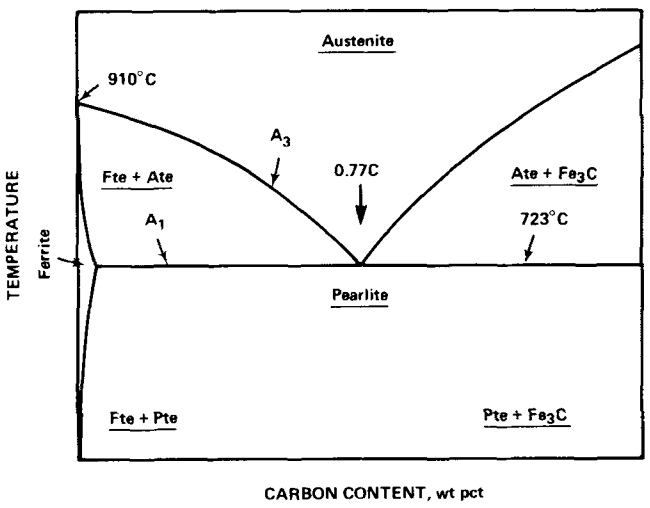

Fig. 1 — Schematic diagram of the phase fields in the neighborhood of the eutectoid temperature in the Fe-C system.

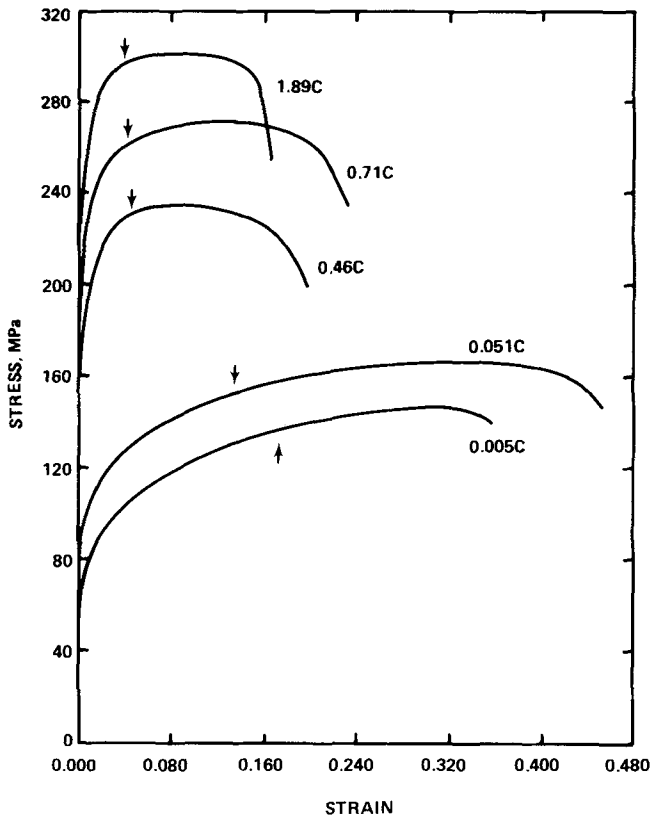

Fig. 2 — Flow curves for 0.001P steels annealed at 1050 °C and deformed at 600 °C. The arrows indicate the strain at the Considére condition, where the force is a maximum. The curves terminate just beyond the onset of necking. Strain rate is 2.3×10^{-2} s^{-1}.

P. J. WRAY is with Inland Steel Company, East Chicago, IN 46312.
Manuscript submitted March 2, 1984.

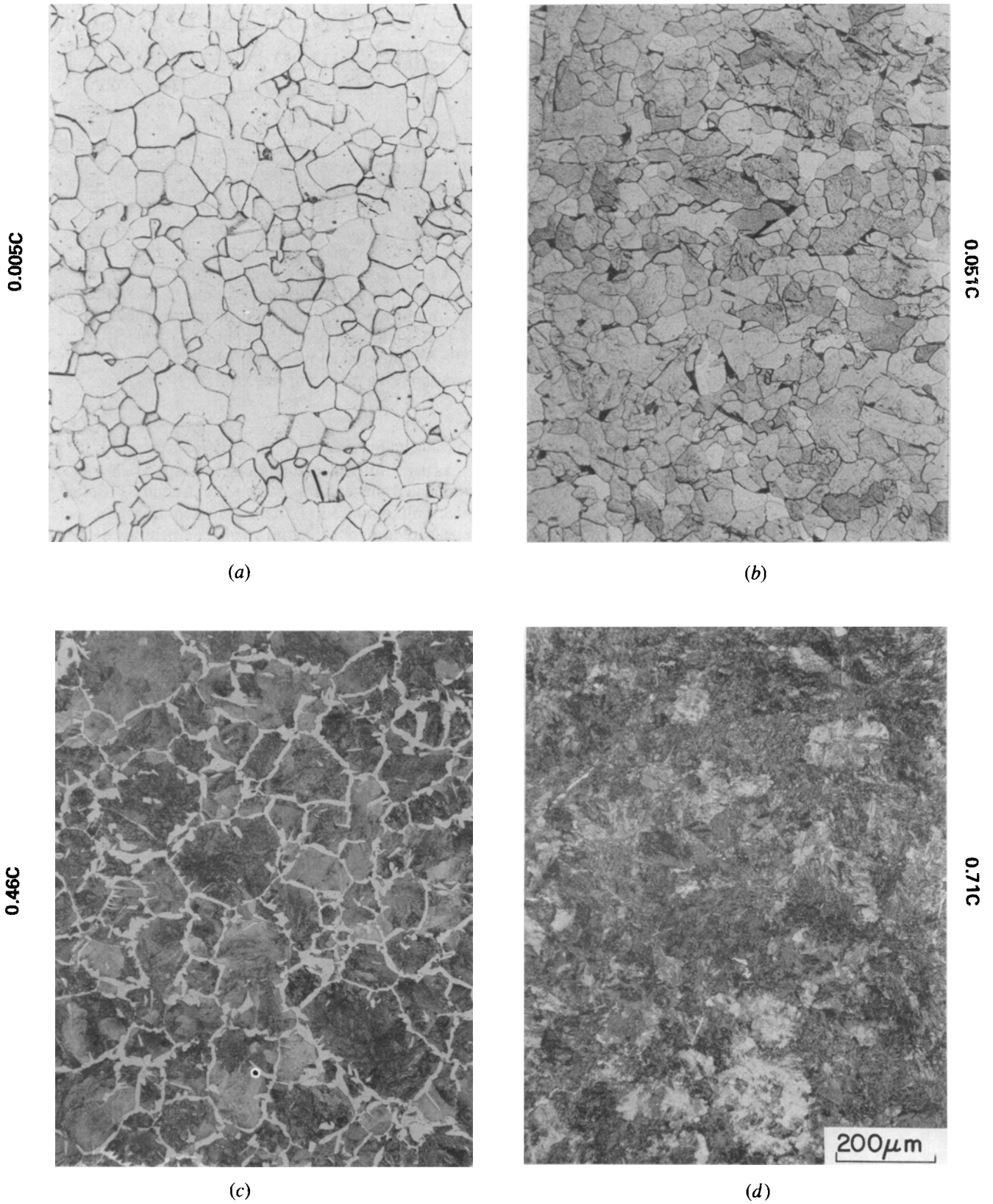

Fig. 3—Microstructures of the hypoeutectoid and eutectoid steels in Fig. 2. Longitudinal sections prepared from the undeformed buttonheads of the tested tension specimens.

to document the plastic flow of these mixtures at temperatures from 500 °C to the eutectoid.

It should be noted at the outset that the documentation of the high-temperature plastic-flow behavior of plain-carbon steels given here is done so primarily for the operator and process designer. As an example of this intent, the possibility of substantial discontinuities in the temperature dependence of the flow stress at the eutectoid temperature will be explored. Moreover, the conditions of which the data are measured are considered to be relatively normal conditions. For example, the microstructures encountered in these experiments are those produced by the moderate cooling rate of 1.5 °C per second at 725 °C. Some variation of these microstructures can be achieved, depending on whether the annealing is being done at very high temperatures to simulate a cast structure, or at, say, 800 °C to produce simple reheating effects; but the effect of such microstructural variations on the flow properties will be shown to be small. Finally, the strain rates used are in the intermediate range up to $2 \times 10^{-2}\ s^{-1}$, but it is expected that most patterns of behavior observed in this range will also hold at higher strain rates.

II. EXPERIMENTAL PROCEDURE

The code letters and chemical compositions of the laboratory-melted materials are given in Table I. The tension-testing procedure was the same as used for previous investigations of the mechanical behavior of austenite.[1,4] Cylindrical button-head type specimens were machined from hot-rolled plate with the tensile axis parallel to the rolling direction. They had a gage-section diameter of 3.2 mm, a diameter-to-gage length ratio of 11.5, and were deformed in an argon atmosphere at true strain rates of 5.5×10^{-6} to $2.3 \times 10^{-2}\ s^{-1}$. Before deformation, the specimens were annealed for one hour either at the deformation temperature, T_D, or at a higher temperature, T_A. In many cases 1050 °C was used as a standard annealing temperature which was low enough for grain growth not to be excessive, but high enough to ensure a fully austenitic structure even for 1.54C. The variation of the austenite grain size with carbon content at 1050 and 1100 °C is given in Table II. There is considerable scatter in the data, with a probable grain size minimum at 0.29C. When annealed at 1100 °C, an increase in grain size is evident at higher carbon levels.

Range of Strain Over Which Flow Stress Is Measured

In the type of tension test used here, measurement of the flow stress is usually possible up to the point where tensile

Table II. Variation of Austenite Grain Size with Carbon Content in 0.8Mn/0.25Si Steels

			Grain Size	
			Average Grain Boundary Intercept, μm	
Code	C, Wt Pct	P, Wt Pct	T_A = 1050 °C	T_A = 1100 °C
E	0.051	0.001	131	114
F	0.29	0.001	47	49, 67
G	0.46	0.001	95	107, 119
H	0.71	0.001	140	170
—	0.67	0.025	—	120, 127
M	0.28	0.170	—	82
N	0.45	0.170	105	110, 112, 120
O	0.65	0.170	158	172
I	0.93	0.015	—	180†
J	1.24	0.016	91	147†
K	1.54	0.015	164	325†
JJ	1.89	0.016	71	350†

†Measured on thermally etched polished surface.

Table I. Chemical Composition of Alloys and Steels Investigated — Weight Percent*

Code	C	Mn	Si	S	P	O
			Fe-Si and Fe-Mn-Si Alloys			
P	0.007	0.011	0.24	0.002	0.001	0.0040
D	0.005	0.85	0.26	0.018	0.001	0.0054
FF	0.005	0.74	0.23	0.023	0.170	0.0156
Q	0.007	1.40	0.25	0.002	0.001	0.0040
R	0.005	0.013	0.95	0.001	0.001	0.0080
S	0.005	1.38	0.94	0.001	0.001	0.0080
			C-Mn-Si Steels			
E	0.051	0.82	0.28	0.018	0.001	0.0069
F	0.29	0.84	0.27	0.018	0.001	0.0053
G	0.46	0.84	0.22	0.029	0.001	0.0033
H	0.71	0.81	0.23	0.028	0.001	0.0020
I	0.93	0.80	0.26	0.024	0.015	0.0030
J	1.24	0.80	0.27	0.024	0.016	0.0016
K	1.54	0.80	0.26	0.025	0.015	0.0009
JJ	1.89	0.82	0.27	0.023	0.016	—
L	0.10	0.74	0.20	0.025	0.170	0.0030
M	0.28	0.72	0.21	0.023	0.170	0.0030
N	0.45	0.74	0.22	0.023	0.170	0.0016
O	0.65	0.74	0.22	0.024	0.170	0.0040

*Residual contents are 0.002N and <0.002Al.

necking begins. Under conditions where the strain rate dependence is small and the material is ductile, the onset of necking usually occurs shortly after the Considére condition $\sigma = d\sigma/d\epsilon$ has been satisfied; however, with respect to the onset of necking at temperatures just below the eutectoid temperature, two observations are worth noting. First, for steels containing mainly ferrite there is a substantial postponement of neck initiation and, therefore, true stress measurements are valid beyond the Considére condition to the point where the stress begins to decrease rapidly, as shown in Figure 2. Second, for steels containing large volume fractions of pearlite, there is no similar postponement of necking. Furthermore, in the mostly-pearlitic steels the Considére condition is reached at small strains, with the result that necking then begins at strains less than 0.15, and the true flow stresses can be measured only over a small range of initial strain.

III. EXPERIMENTAL RESULTS

Before considering the plastic flow behavior of the mixtures, the plastic-flow characteristics of the individual components of the ferrite + pearlite mixture will be examined separately.

A. *High Temperature Behavior of the Ferrite Phase*

Stress-strain data over the temperature range 600 °C to 1300 °C are presented in Figure 4 for the Fe-0.24Si binary alloy P deformed at the rate of 2.3×10^{-2} s^{-1}. There is a clear strength difference between the bcc ferrite and the stronger fcc austenite at all strain levels, and the difference increases with strain. Because of its low alloy content, particularly carbon content, this material exhibits a narrow temperature range, between 900 and 950 °C, in which austenite and ferrite coexist. The results at 925 °C indicate that within this region a portion of the initial ferrite may transform to austenite during deformation.

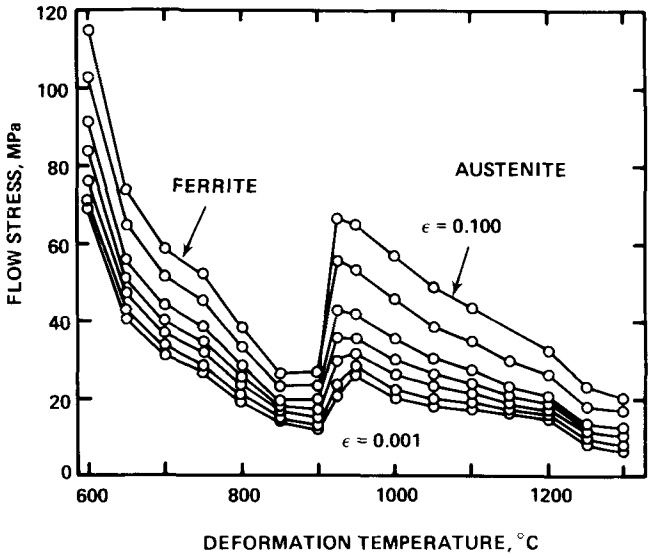

Fig. 4—Temperature dependence of the flow stress of the reference Fe-0.24Si alloy P, illustrating the relative strengths of the ferrite and austenite phases at strain levels of 0.001, 0.002, 0.005, 0.01, 0.02, 0.05, and 0.10. Annealing condition $T_A = T_D$.

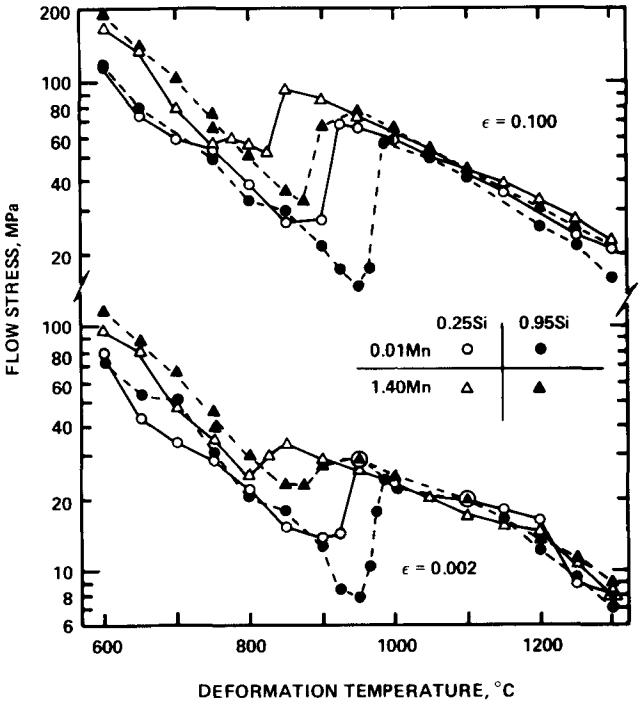

Fig. 5—Strengthening effect of Mn and Si in the ferrite and austenite phases of 0.005C steels P, Q, R, and S. Annealing condition $T_A = T_D$.

The effect of adding manganese and increasing the silicon content of the Fe-0.24Si alloy is shown in Figure 5. Here the logarithm of the flow stress at strain levels of 0.002 and 0.100 is plotted against deformation temperature over the range 600 to 1300 °C for steels P, Q, R, and S. Manganese appears to have a greater strengthening effect than does silicon. Manganese also stabilizes the austenite and, therefore, lowers the transformation temperature. Because the temperature dependence of the flow stress is less in austenite, this shift reduces the change in the flow stress at the transformation. Silicon is a ferrite stabilizer and has the opposite effect on the flow stress change at the transformation. Furthermore, although the temperature range of the austenite + ferrite region shifts with manganese and silicon content, the range remains narrow in these 0.005C steels, and the sharp change in flow stress which accompanies the phase transformation must be treated as a discontinuity.

Another characteristic of the plastic-flow behavior is the work-hardening exponent n_m, where n_m is the maximum value of $d(\log \sigma)/d(\log \epsilon)$ usually measured at a true strain in the vicinity of 0.05. Measurements of n_m in Figure 6 for the same steels as in Figure 5 clearly show the difference in work hardening for the two phases, as well as the sharp transition in behavior at the transformation temperature. The lower rate of work hardening for ferrite indicates that dynamic recovery is greater in ferrite than in austenite. This agrees with the explanation that because dynamic recovery is easier in ferrite, the competing recovery process of dynamic recrystallization rarely occurs in ferrite but readily does so in austenite.

The data in Figure 5 show that changes in alloy content have a stronger effect on the strength of ferrite than on that of austenite. The effect of alloying on the ferrite strength is further illustrated in Figure 7, where the relative change in

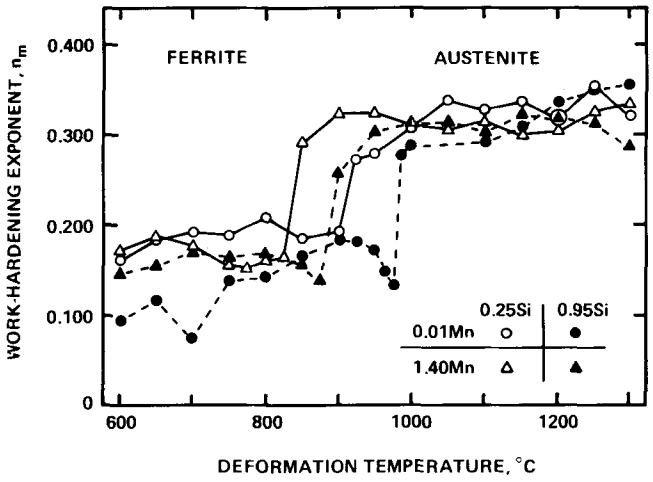

Fig. 6—Temperature dependence of the work-hardening exponent $n_m = d(\log\sigma)/d(\log\epsilon)$ for the steels used in Fig. 5.

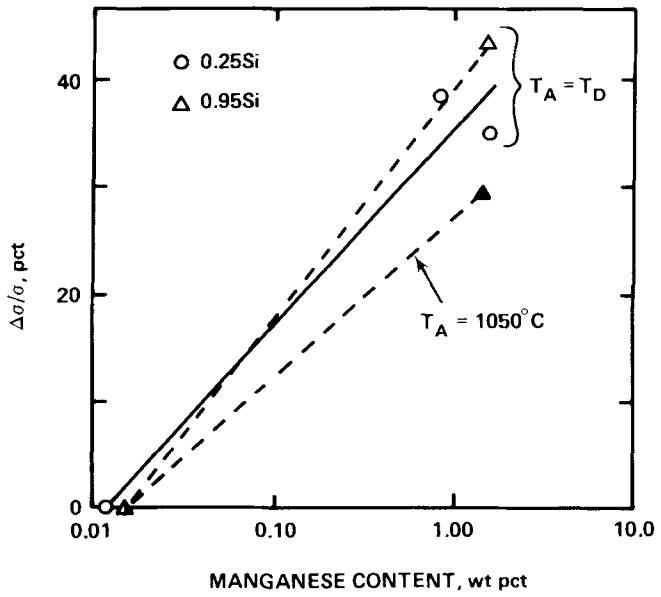

Fig. 7—Relative increase in the 0.002 yield stress of Fe-0.24Si alloy P and Fe-0.95Si alloy R with the addition of manganese. T_D = 600 °C.

the yield stress of the reference binary alloys P and R is plotted as a function of manganese content. The addition of one weight percent manganese produces a relative increase in yield stress of about 40 pct at 600 °C. This increase is independent of the silicon content but is less for the annealing condition of T_A = 1050 °C. The strong dependence of the flow stress of ferrite on solute content was discussed by Leslie.[9] That manganese has a greater strengthening effect than does silicon (Figure 5) may be due in part to the fact that manganese tends to refine the ferrite grain size, whereas silicon coarsens it as shown in Table III.

An even greater strengthening effect than that of Mn or Si is indicated in Figure 8, where the flow stresses

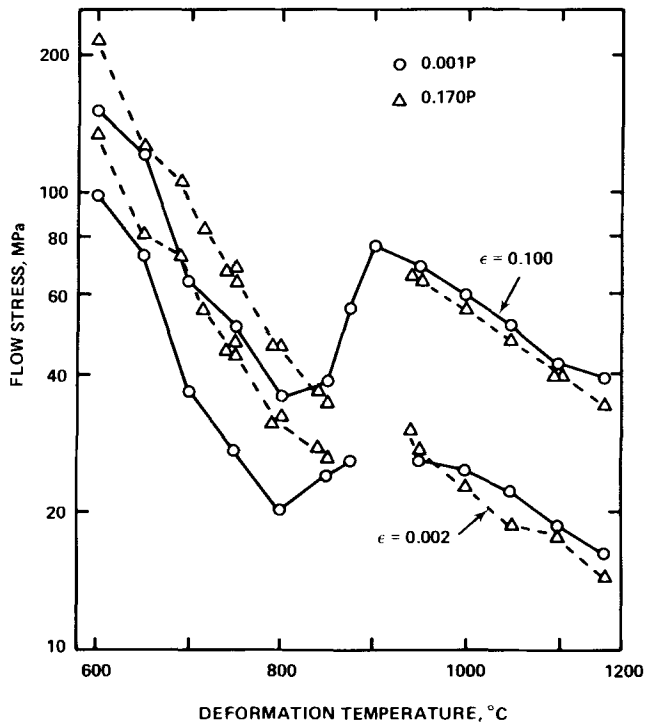

Fig. 8—Strengthening effect of phosphorus on the ferrite and austenite phases in 0.005C/0.8Mn/0.25Si steels D and FF. Annealing condition $T_A = T_D$.

Table III. Effect of Annealing Temperature and Composition on Ferrite Grain Size in 0.005C Steels

		Average Grain Boundary Intercept, μm					
Annealing Temp., °C	Mn	0.011	0.013	0.85	0.74	1.40	0.38
	Si	0.24	0.95	0.26	0.23	0.25	0.94
	P	0.001	0.001	0.001	0.170	0.001	0.001
600		82, 97	113	37	55	40	52
650		85, 90	157, 185	41, 53	—	47	45, 62
700		74, 80	192	83, 90	58	54	45
750		78, 79	179	136	—	51, 56	51
800		90, 101	195	126	55	58	83
850		527, 721	134	66	—	49, 62	208, 310
900		330, 401	—	69	62	50	—
950		100	480		—	51	96
1000		—	314		—	64	116
1050		94	260, 380	56	110	92	56
1100		—	364	98	—	83, 92	66
1150		108	390	112	—	69	232
1200		129	545	119	—	77	226
1250		191	553	102, 116	—	93	296
1300		—	422	119	—	110	239

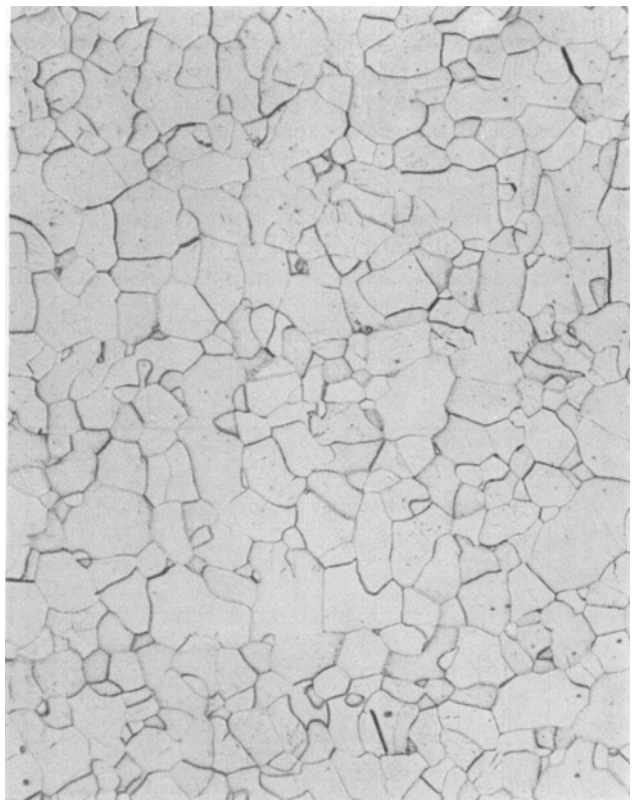

(*a*)

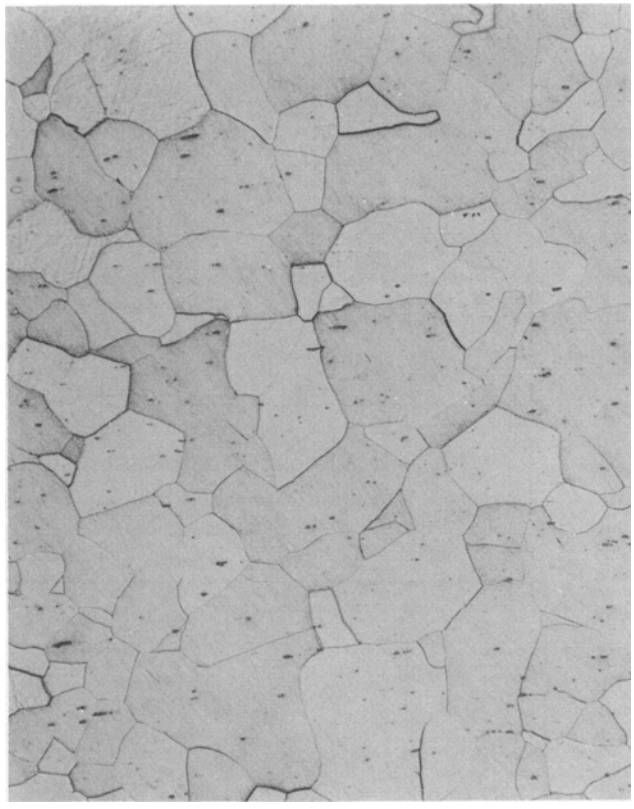

(*b*)

0.001P

(*c*)

0.170P

(*d*)

Fig. 9—Grain structure of 0.001P steel D and 0.17P steel FF after annealing for 1 h at 1050 °C (*a*), (*b*) or at 600 °C (*c*), (*d*).

of 0.005C/0.8Mn/0.24Si steels containing 0.001P and 0.170P are compared. The substantial strengthening of ferrite by phosphorus is in strong contrast to the softening observed in austenite.[10] In the latter case softening is partially due to the enhanced grain coarsening of austenite produced by phosphorus. This austenite grain coarsening has a residual effect on the subsequent ferrite grain structure, so that the ferrite grains are coarser in the higher phosphorus steel as shown in Figure 9; however, in ferrite the softening associated with the larger grain size is not sufficient to counter the solution hardening effect of phosphorus.

The influence of annealing condition on the plastic flow of ferrite at 600 °C is illustrated in Figure 10 for the 0.005C steels D and FF. In the case of the low-phosphorus steel D, prior annealing in the ferrite range produces substantial recovery plus some grain growth, as illustrated by the grain size measurements in Figure 11. A similar occurrence of rapid ferrite grain growth just below the transformation temperature of 0.005C steels was also measured for steels P, R, and S and is recorded in Table III. Annealing just above the transformation temperature results in a finer grain structure (Figure 11) which counters the recovery effects and causes an increase in strength (Figure 10). Only after annealing at temperatures greater than 1200 °C is there an indication in Figure 10 of large-grain-structure softening. In the case of the high-phosphorus steel, the strengthening at 600 °C due to phosphorus is substantial and is independent of the annealing condition up to T_A = 1050 °C.

Finally, the strain rate dependence of the flow stress of ferrite at 600 and 850 °C is presented in Figure 12(a) for the 0.005C/0.8Mn/0.25Si steel D. The strain rate exponent measured for the yield stress is 0.121 at 600 °C and 0.189 at 850 °C. The strain rate sensitivity is considerably less in the austenite phase, where at 950 °C an exponent value of 0.088 was measured for the same steel.

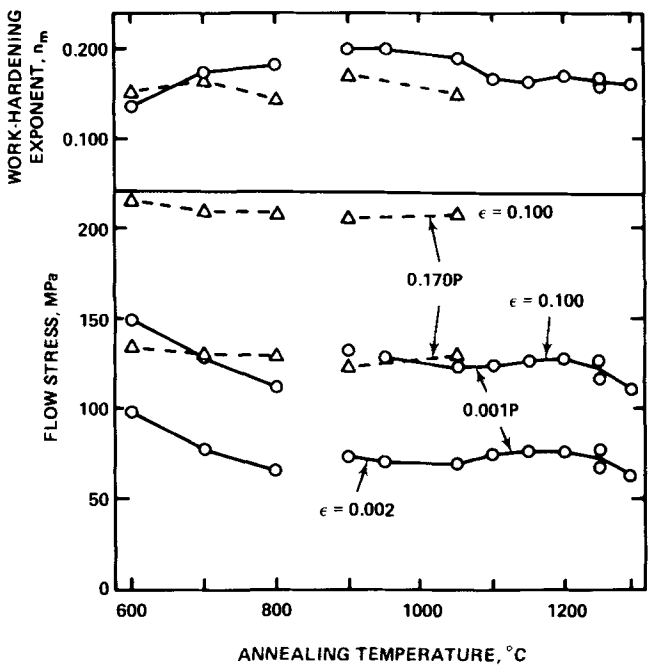

Fig. 10—Variation of plastic flow behavior at 600 °C with annealing temperature. Steel D (0.001P) and steel FF (0.17P).

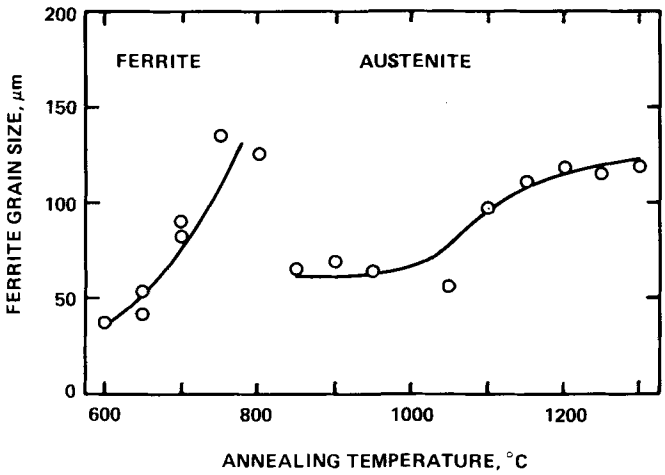

Fig. 11—Annealing temperature dependence of the ferrite grain size, represented by the average grain boundary intercept. Note the occurrence of grain growth when annealed at high temperatures in the ferrite region. 0.005C steel D.

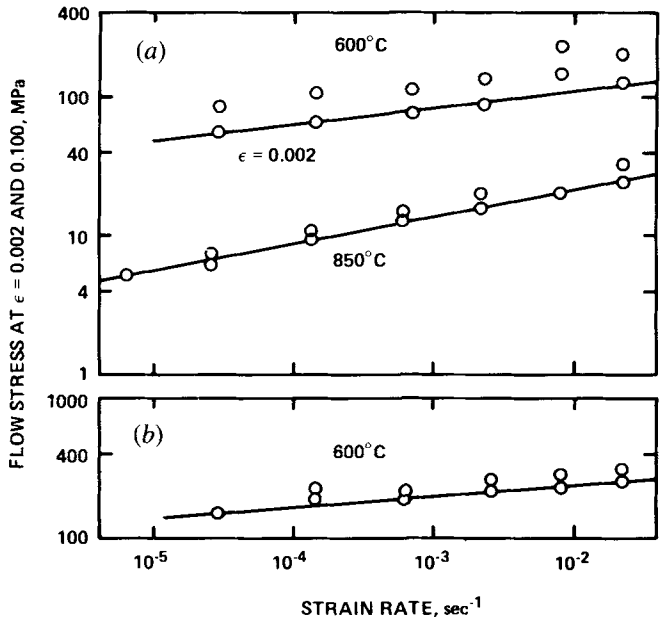

Fig. 12—Strain rate dependence of the flow stress at ϵ = 0.002 and 0.100. (*a*) 0.005C steel FF in the ferrite region at 600 °C and 850 °C and (*b*) 0.65C steel O in the pearlite region at 600 °C ($T_A = T_D$).

B. *High Temperature Behavior of Pearlite*

The temperature dependence of the plastic flow of two steels which are close to the eutectoid composition, but which have different phosphorus contents, is shown in Figure 13. The discontinuity at the eutectoid temperature is due to the difference in behavior of austenite and pearlite. As Sherby and co-workers[11] observed earlier, the discontinuity is not large when the flow stress is plotted on a logarithmic scale and measured at large strains. The new observation here is that at small strains the flow stress of pearlite is much higher than that of austenite; it is only because the lower yield stress of austenite is balanced by the high rate of work hardening (Figure 14) that the small flow stress discontinuities were previously observed at larger strains.

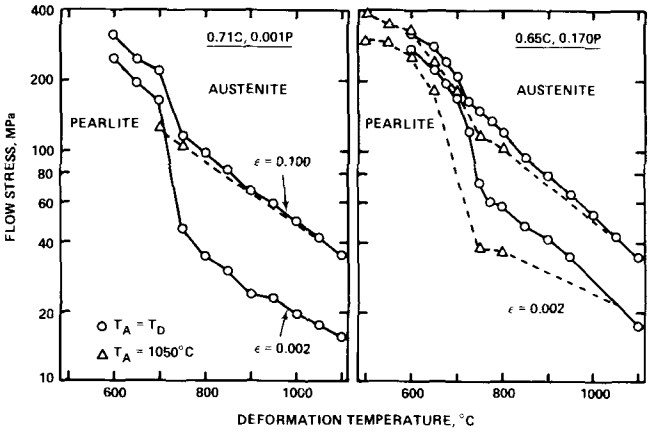

Fig. 13—Temperature dependence of the flow stress of eutectoid steels H and O. Annealing condition $T_A = T_D$.

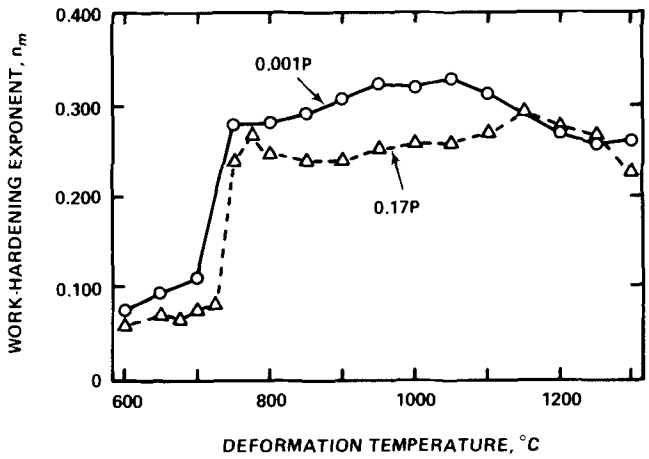

Fig. 14—Variation of the work-hardening exponent n_m with temperature for the steels H and O used in Fig. 13.

Examples of the structure of the pearlite in the eutectoid steels are given in Figure 15. In an effort to account for the influence of phosphorus on the flow behavior of eutectoid steel, shown in Figures 13 and 14, the interlamellar spacing of the pearlite was measured. Cooling the 0.001P steel H from 1050 °C, where the austenite grain size is about 140 μm (Table II), at a standard cooling rate which is about 90 °C per minute at the transformation temperature, produced an average true interlamellar pearlite spacing of 0.3 μm.* After measuring the pearlite interlamellar spacing of the 0.17P steel O, it was concluded that if there was an influence of phosphorus on the interlamellar spacing, it was small, and would require an extensive statistical analysis to resolve.

*Assuming parallel plane lamellae in randomly oriented colonies, the average true center-to-center spacing is half the average interlamellar spacing measured on a random test secant.[12]

An additional aspect of the pearlitic microstructure is the stability during deformation, and the effect structural instability may have upon the plastic flow behavior. For example, it is known that in the presence of an applied stress, the lamellar structure may fragment and degenerate to a globular cementite structure.[13,14,15] Such a morphological change during deformation could lead to a lowering of the maximum flow stress at low strain rates where there is sufficient time for the strain accelerated degeneration to occur. Accordingly, an examination was made of the deformed pearlite structure in eutectoid steels deformed at lower strain rates.

The structure in the necked region of a specimen deformed at a rate of 6.5×10^{-4} s^{-1} is shown in Figure 15(c). Here the strain is a little more than 0.20 and was produced in about 300 seconds at a stress level of 200 MPa. The majority of pearlite colonies present showed no evidence of degeneration, suggesting that no major change in flow properties due to structural instability should be expected for eutectoid steels processed at strain rates faster than 6×10^{-4} s^{-1}.

The strain rate dependence of the flow stress of pearlite at 600 °C is shown in Figure 12(b). The measured value of the strain rate exponent for the 0.002 yield stress is 0.074, and this low value can be compared with 0.121 for ferrite at the same temperature. Thus, pearlite is not only stronger than ferrite at intermediate strain rates, but its strength is less dependent on strain rate than is the strength of ferrite.

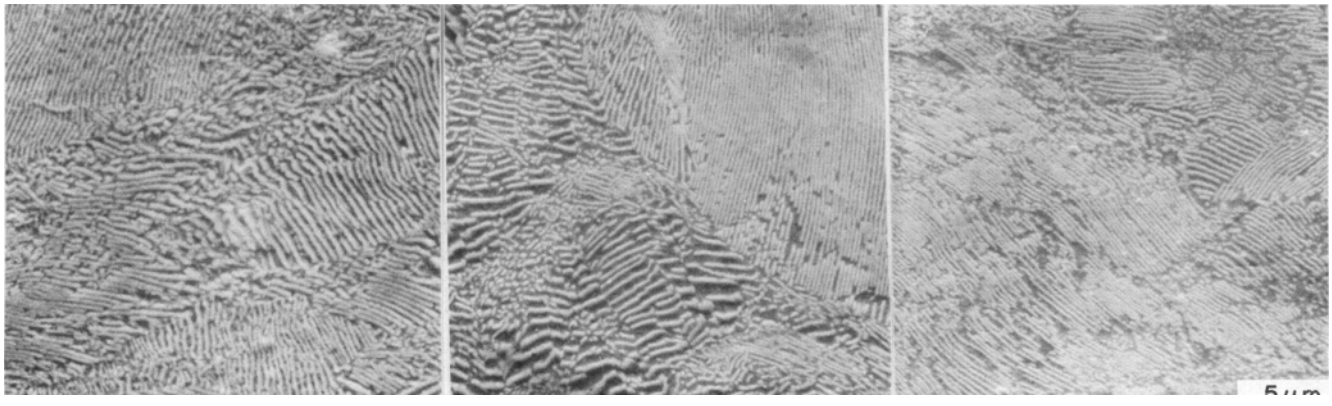

(a) (b) (c)

Fig. 15—Illustration of pearlite morphology in eutectoid steels H and O. Cooling rate at the eutectoid temperature is 1.5 °C/second.

C. *Ferrite + Pearlite Mixtures*

The strong carbon dependence of the flow stress at 600 °C of these mixtures as produced after annealing at 600 and 1050 °C is shown in Figures 16 and 17, respectively, and the variation in microstructure is shown in Figure 18. As could have been noted above, the fully pearlitic steels are more than twice as strong as the fully ferritic steels. The strength, therefore, increases continuously with carbon content across the ferrite plus pearlite range although after annealing at 1050 °C (Figure 17) there is a suggestion that the strength saturates at about 70 pct pearlite. Similar behavior was observed for specimens deformed at 650 and 700 °C.

While the strength of the ferrite plus pearlite mixture increases with increasing carbon content and, therefore, with increasing volume of pearlite, the Considére strain and the strain at the onset of necking decrease as indicated in Figure 2. The observed decrease in Considére strain ε_c is in accord with the decline in the work-hardening exponent n_m shown in Figure 17(b), recalling that for power-law work hardening the exponent n_m is equivalent to ε_c. With regard to the work hardening behavior, it should be noted that, if instead of measuring the maximum value of exponent n at strains of about 0.05, the rate of work hardening $d\sigma/d\varepsilon$ is measured at 0.002 strain, then this different index of work hardening actually increases with carbon content from about 4 GPa at 0.005C to about 8 GPa at 0.7C.

As the strength of the ferrite + pearlite mixture increases with carbon content below the eutectoid temperature, the strength of the austenite phase above the eutectoid decreases.[4] Therefore, as the carbon content increases, a sharp flow-stress transition is created at the eutectoid temperature, as shown by the set of stress-temperature curves in Figure 19. In the case of the 0.10C steel the flow-stress transition at the eutectoid is partly masked by having the ferrite + austenite mixture above the eutectoid temperature. In addition, it apparently makes little difference whether or not the 0.10C steel is pre-annealed at 1050 °C in the austenite region.

In the 0.45C and 0.65C steels the larger amounts of pearlite raise the flow stress at temperatures below the eutectoid, and the flow-stress discontinuity at the eutectoid temperature is seen to be substantial.*

*The absence of flow stress values at $\varepsilon = 0.002$ in the austenite region of the higher carbon steels is due to the occurrence of a yield point phenomenon previously observed at temperatures above 850 °C.[16]

A more detailed examination of the effect of phosphorus addition, initial hot-rolled structure, and annealing treatment on the plastic flow of a ferrite + pearlite mixture is illustrated in the series of Figures 20 to 22 for the 0.45C steels G and N. The temperature dependence of the flow stress at 0.002 and 0.100 strains is given in Figure 20 for specimens prior annealed at 1050 °C. The strengthening effect of the 0.17P addition is substantial in the temperature range of the ferrite + pearlite mixture, but diminishes with temperature in the austenite. The same influence of phosphorus was observed for the annealing condition $T_A = T_D$. Because the effect of phosphorus on the ferrite + pearlite mixture may be related to a possible phosphorus-induced difference in prior austenite grain size, the grain

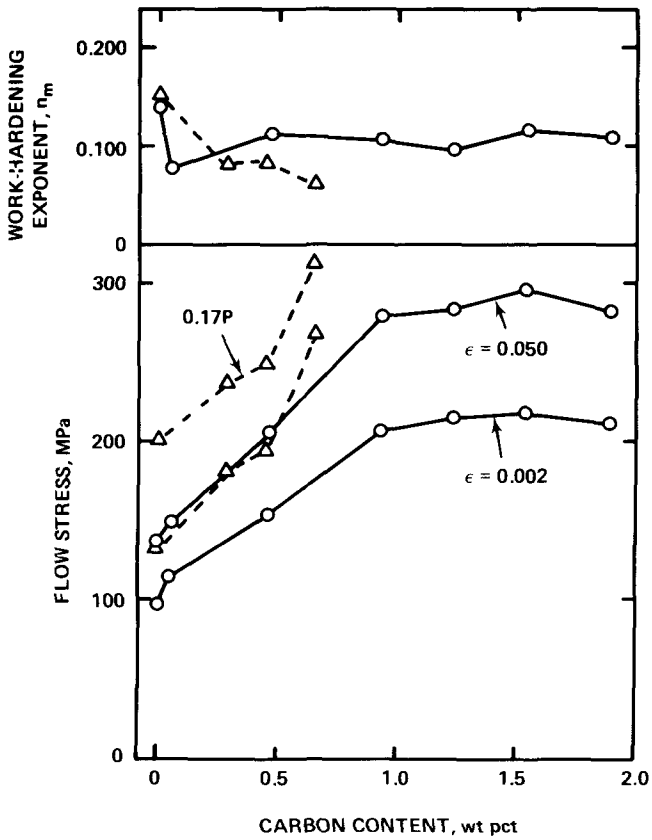

Fig. 16—Variation of the plastic flow behavior at 600 °C with carbon content. Annealing condition $T_A = T_D$.

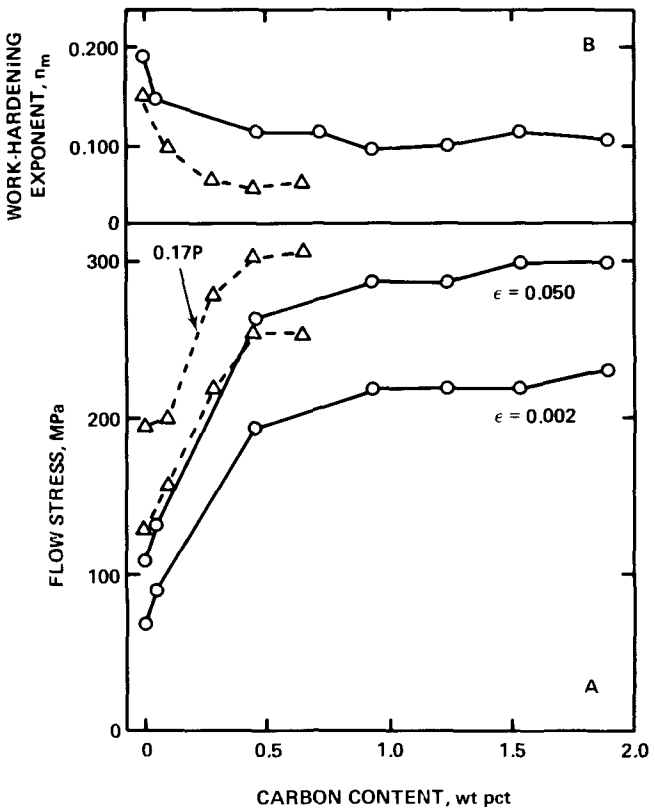

Fig. 17—As for Fig. 16, but with the annealing condition T_A = 1050 °C.

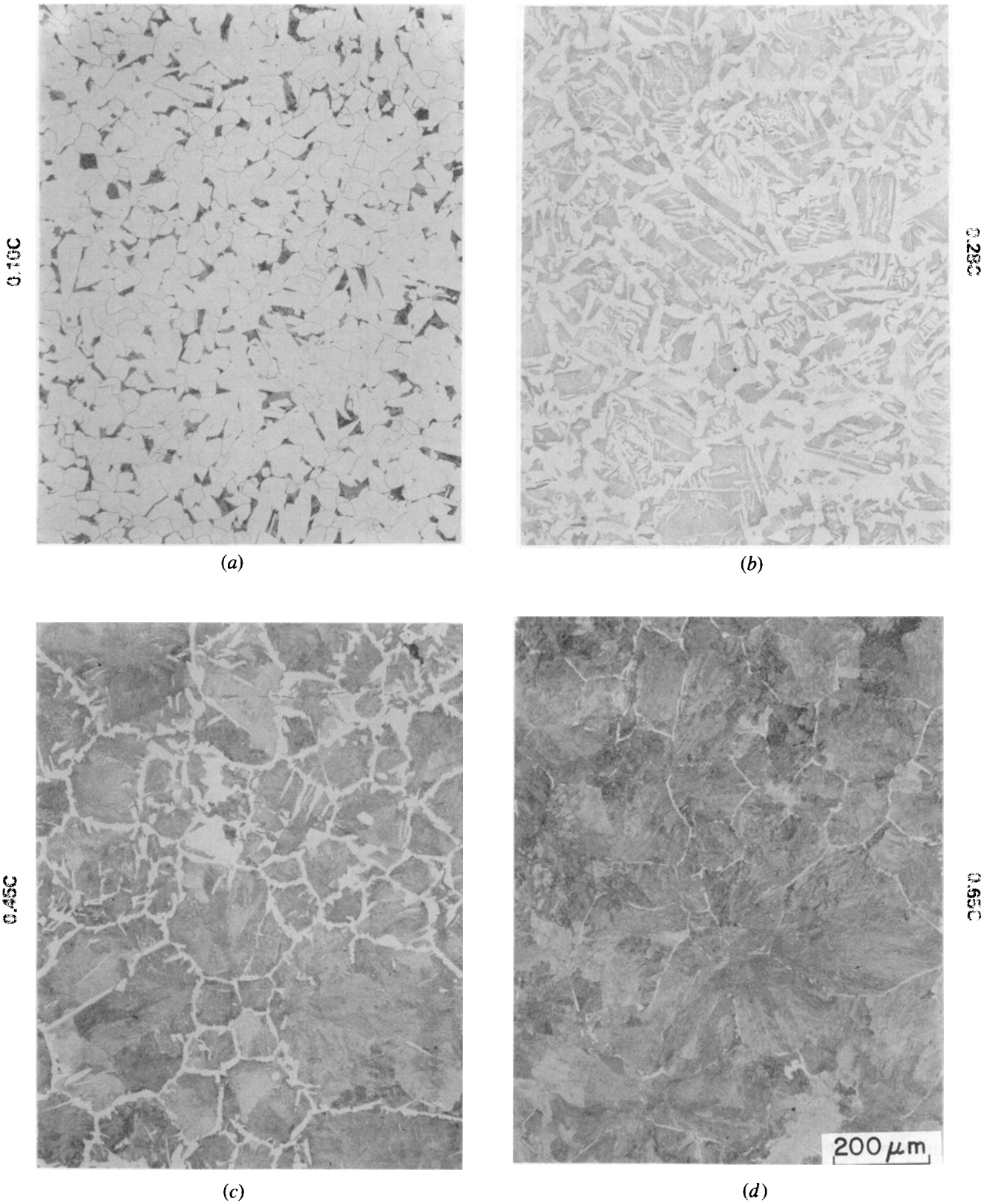

Fig. 18—Microstructures of the 0.17P hypoeutectoid steels L-O annealed at 1050 °C. Compare with Fig. 3.

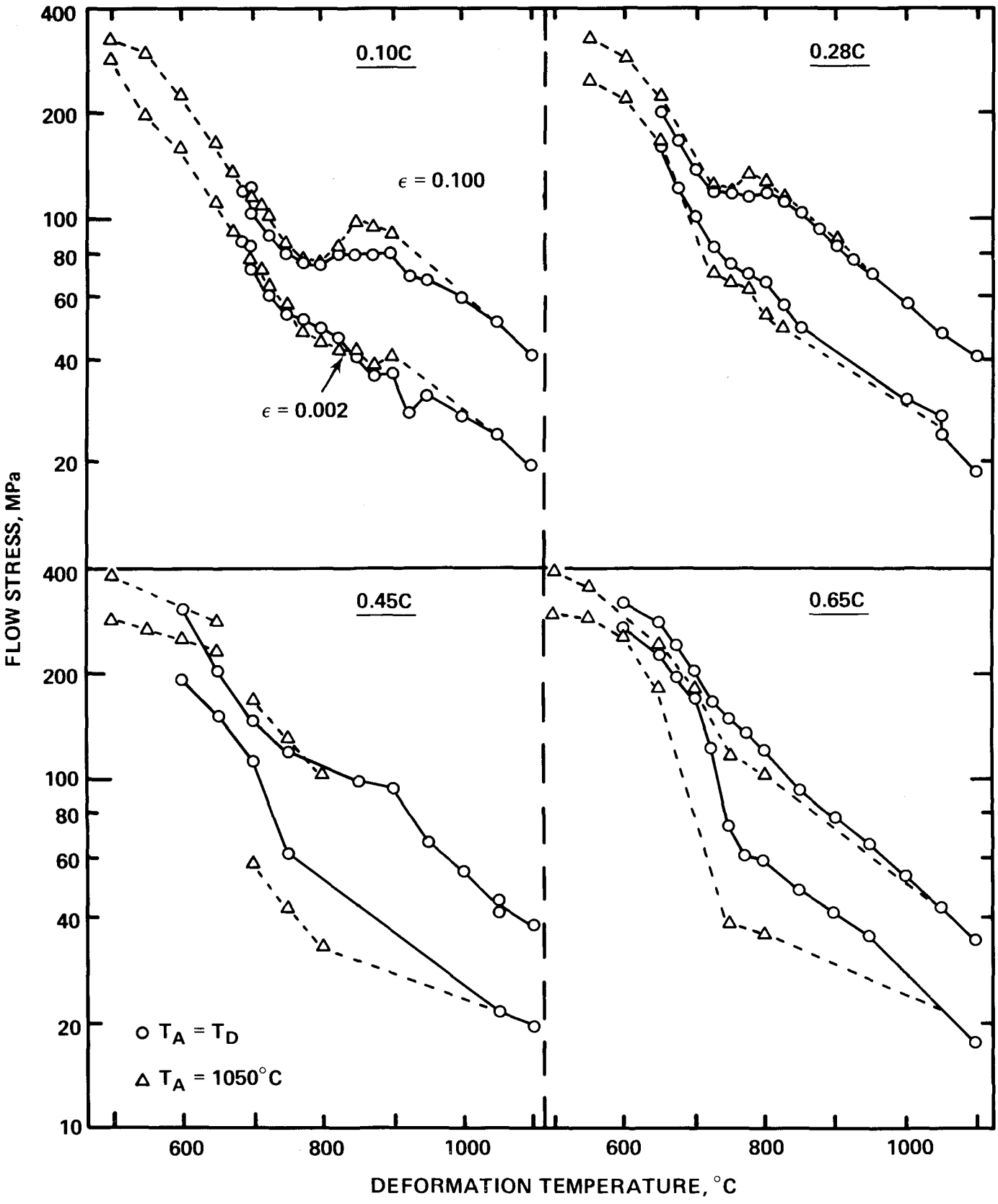

Fig. 19—Temperature dependence of the flow stress of 0.17P hypoeutectoid steels L-O, showing the discontinuity in flow stress at the eutectoid temperature.

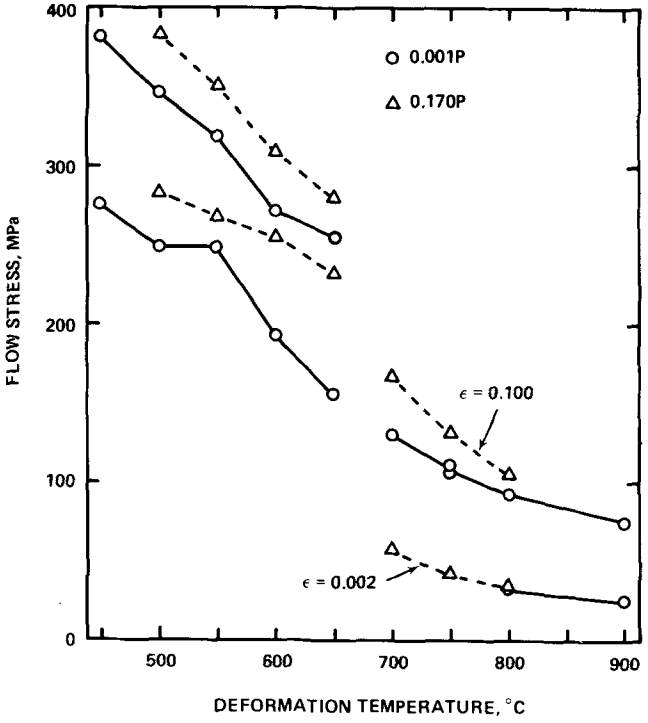

Fig. 20—Variation of the flow stress of 0.45C steels G and N with temperature in the ferrite + pearlite, austenite + ferrite, and austenite regions. Annealing condition T_A = 1050 °C.

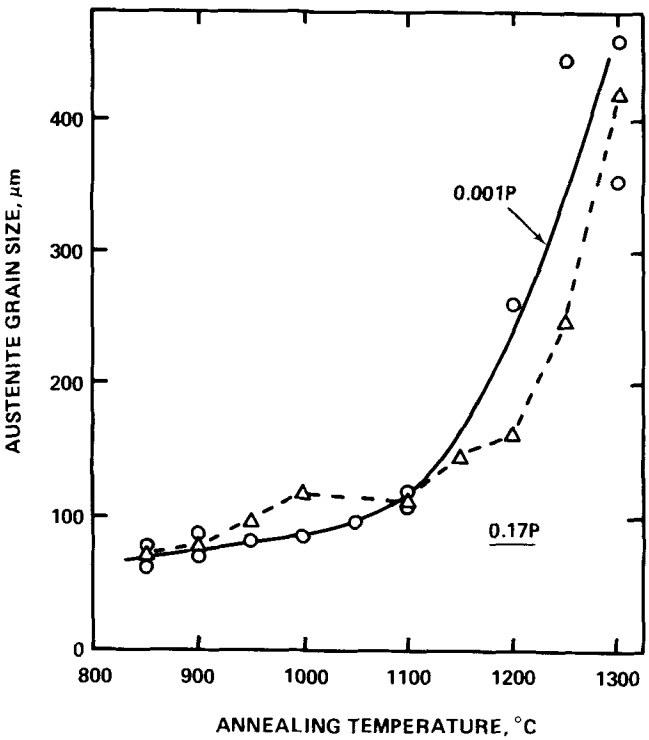

Fig. 21—Variation of the austenite grain size with annealing temperature in the 0.45C steels G and N. Annealing period is 1 h.

growth characteristics of the two 0.45C steels were measured and the results are shown in Figure 21. Evidently there is no significant effect of phosphorus on the grain growth of 0.45C steels.

To explore the effect of microstructure on the plastic flow of 0.001P steel G at 600 °C, the temperature of prior-

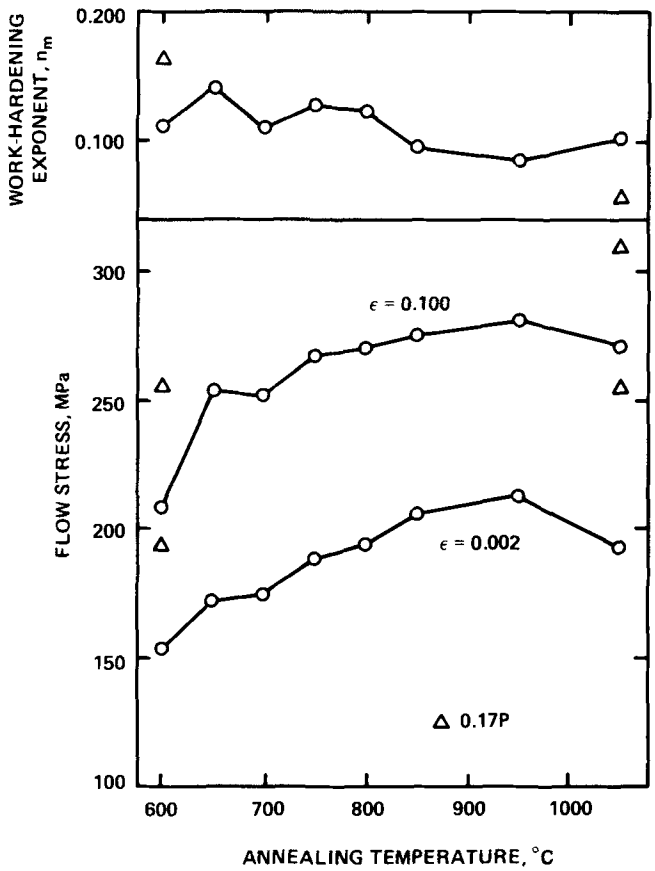

Fig. 22—Annealing temperature dependence of the plastic flow behavior of 0.46C steel G at 600 °C.

annealing was varied and the results are given in Figure 22. The flow stress increased with increasing annealing temperature until grain growth softening began at some temperature above 950 °C. The variations in microstructure for the 0.001P steel are shown in Figure 23. After annealing at 650 and 700 °C a very fine grained, banded structure of ferrite and pearlite remains from the prior hot-rolled plate processing, with banding being more evident at 700 °C. Annealing at 750 °C in the austenite + ferrite region for one hour produced some breakup of the banded structure, but only by annealing in the austenite region, as at 850 °C, is the banded structure completely removed. These structural changes do not account for the increase in strength recorded in Figure 22. Furthermore, the increase is contrary to the initial decrease in flow stress shown for 0.005C steels in Figure 10.

The initial structures of the 0.17P steel at 650 and 700 °C, shown in Figure 24, are quite different from those of the 0.001P steel shown in Figure 23. The prior austenite grain size is much larger for the 0.17P steel, and there is no evidence of banding in the ferrite, proeutectoid ferrite, and pearlite mixture. Annealing in the austenite + ferrite region at 750 °C produces a complex and slightly banded structure, but annealing at 850 °C in the austenite region results in a structure similar to that of 0.001P also annealed at 850 °C.

D. *Pearlite + Cementite Mixtures*

From the assumed eutectoid composition of 0.77C to 1.89C the volume fraction of cementite increases from

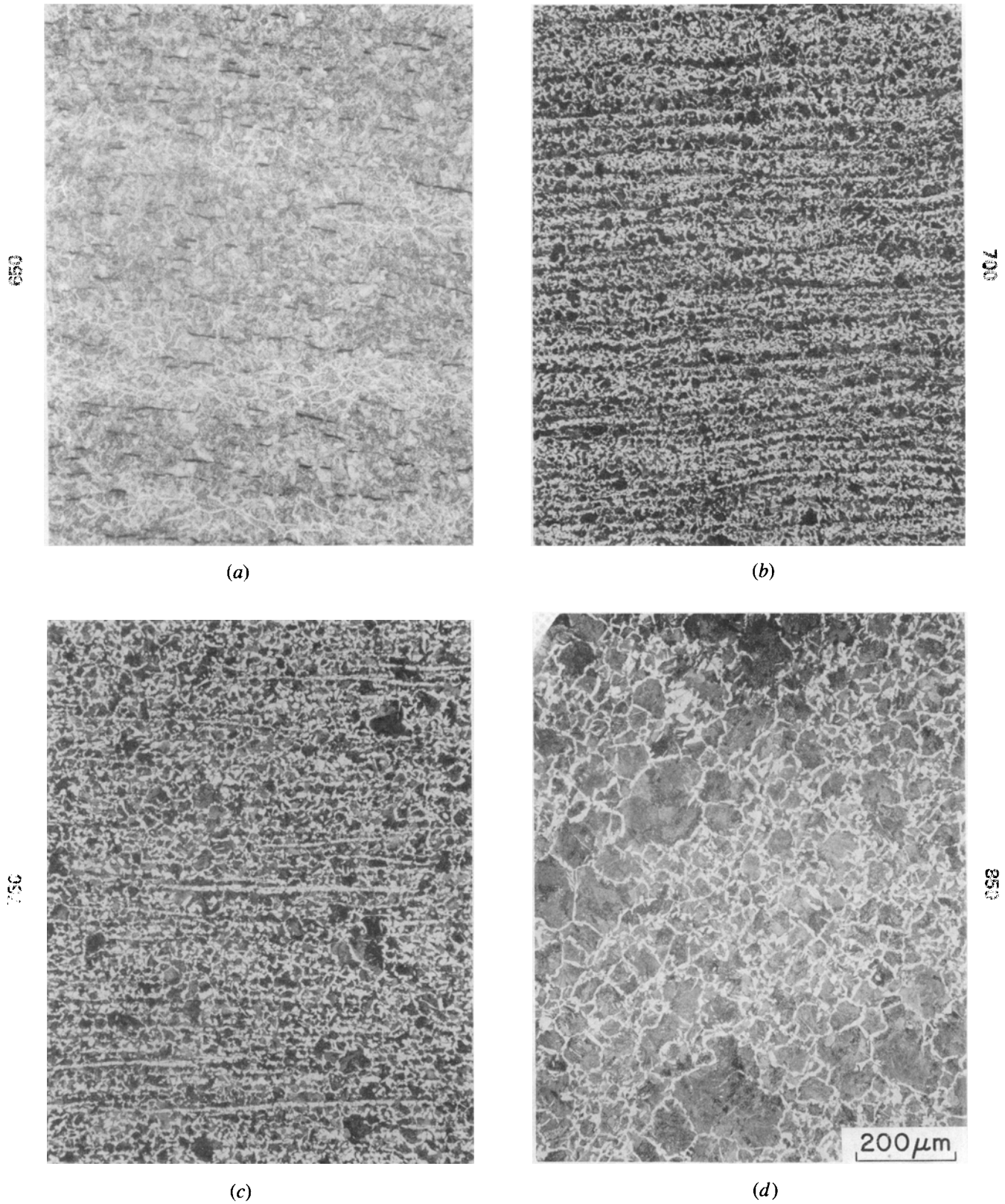

Fig. 23 — Microstructure of 0.46C steel G (0.001P) after annealing at temperatures below, in, and above the austenite + ferrite region ($T_A = T_D$).

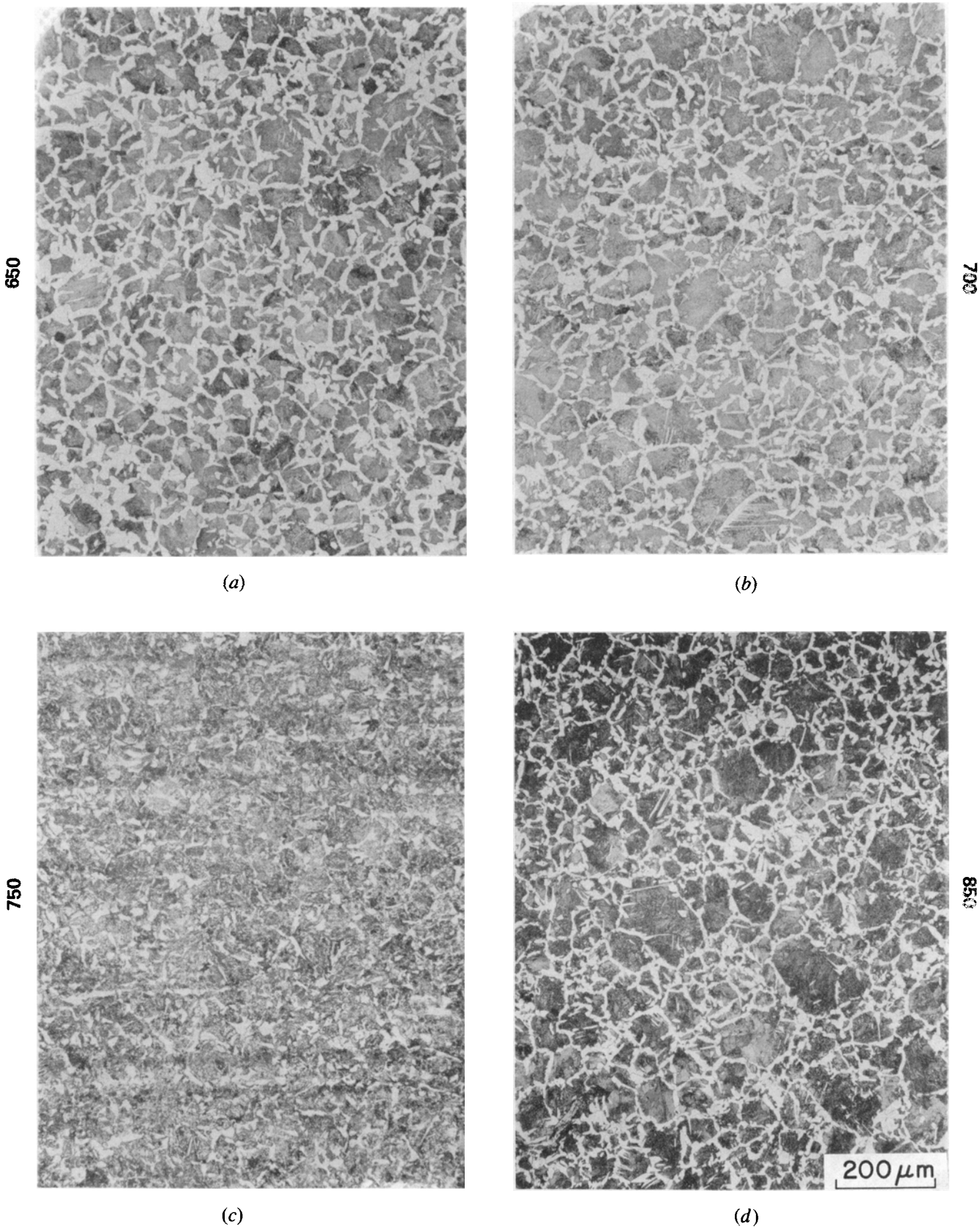

Fig. 24 — Microstructure of 0.45C steel N (0.17P) annealed at the same temperatures as in Fig. 23.

12 pct to 29 pct, as estimated from the Fe-C phase diagram.* At 600 °C the deformation behavior of this mixture

*The volume fraction f of β in an $\alpha + \beta$ mixture is given by

$$f = \left[1 + \frac{\rho_\beta}{\rho_\alpha}\left(\frac{1}{g} - 1\right)\right]^{-1}$$

where g is the mass fraction from the lever rule and ρ is the density. The density of the austenite, cementite, and ferrite components is given in Table IV. For the ferrite + cementite mixture the density ratio is almost unity, so that the volume fraction is approximately equal to the mass fraction.

is practically independent of carbon content over the range 0.93 to 1.89C, as shown in Figures 16 and 17. Evidently the strength of the pearlite and cementite are comparable enough that the proportion of their admixture does not affect the plastic flow behavior. That the flow behavior of this mixture varies only slightly with deformation temperature over the range 500 to 650 °C is shown in Figures 25 and 26 for the 1.54C and 1.89C steels.

Comparison of the flow stress data in Figures 16 and 17 indicates that the plastic flow behavior is similar whether prior annealing is done at 600 or 1050 °C. This is somewhat surprising because, as shown in Figure 27, the microstructures produced by the two annealing procedures are quite different. Annealing the hypereutectoid steels at 600 °C does not remove the prior banded hot-rolled structure similar to that found in the low-phosphorus eutectoid steel. However, annealing at 1050 °C in the austenite range produces a large grain structure (Table II) with an abundance of Widmanstätten cementite (Figure 27(b)). If at 1050 °C the austenite + cementite region is entered, the resulting structure then includes proeutectoid cementite (Figure 27(c)).

E. *Austenite + Cementite Mixtures*

The stress-temperature curves for the two hypereutectoid steels in Figures 25 and 26 show that there is no marked discontinuity in flow stress at the eutectoid temperature, although in the austenite + cementite region the stress falls sharply with increasing temperature. A bigger difference in plastic flow behavior of the phases is indicated by the measurements of the work-hardening exponent n_m in Figure 28.

The results in Figure 28 also show that as the carbon content increases in the austenite + cementite region above the eutectoid temperature, the work-hardening exponent decreases appreciably. The estimated volume fraction of cementite in this mixture at 725 °C is 13 pct for the 1.54C steel

Table IV. Density of Mixture Components

Temperature, °C	Density, g/cm³		
	Ferrite	Austenite at 0.77C	Cementite
RT	7.874[a]	—	7.681[c]
600	7.681[a]	—	7.531[c]
725	7.642[a]	7.576[b]	7.479[c]

References (a) L. D. Lucas: *Mem. Sci. Rev. Mét.*, 1972, vol. 69, pp. 479-92.
(b) N. Ridley and H. Stuart: *Metal Sci. J.*, 1970, vol. 4, pp. 218-22.
(c) H. Stuart and N. Ridley: *JISI*, 1966, vol. 204, pp. 711-17.

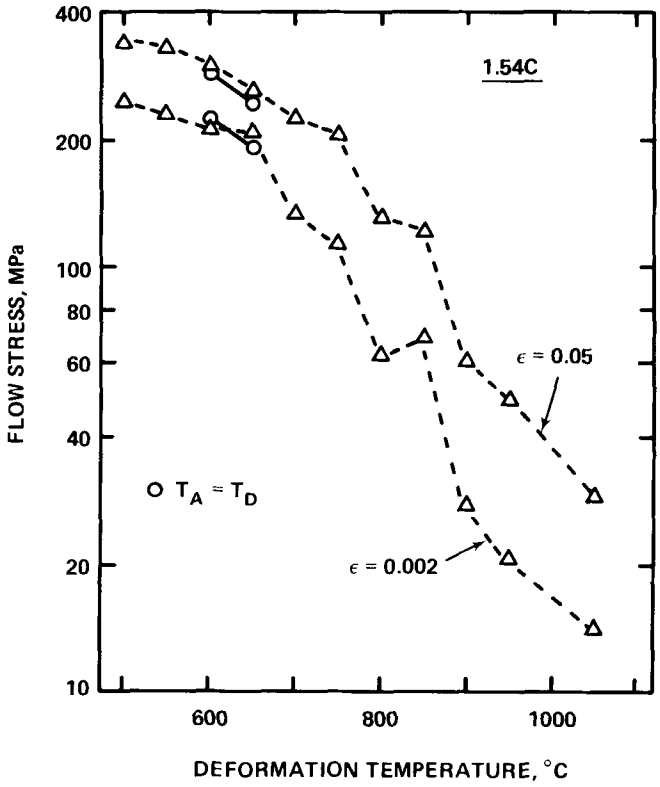

Fig. 25—Variation of the flow stress with temperature for the 1.54C hypereutectoid steel K. Annealing condition T_A = 1050 °C.

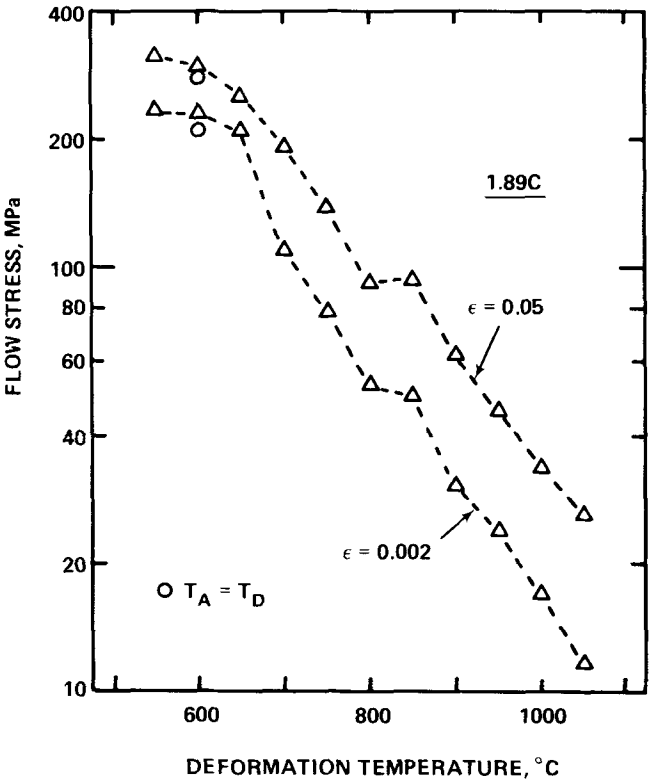

Fig. 26—Variation of the flow stress with temperature for 1.89C hypereutectoid steel JJ. Annealing condition T_A = 1050 °C.

and 19 pct for the 1.89C steel. As the amount of cementite decreases with increasing temperature, the work hardening behavior approaches that of the austenite phase, which is exemplified by the data for the 0.71C steel in Figure 28.

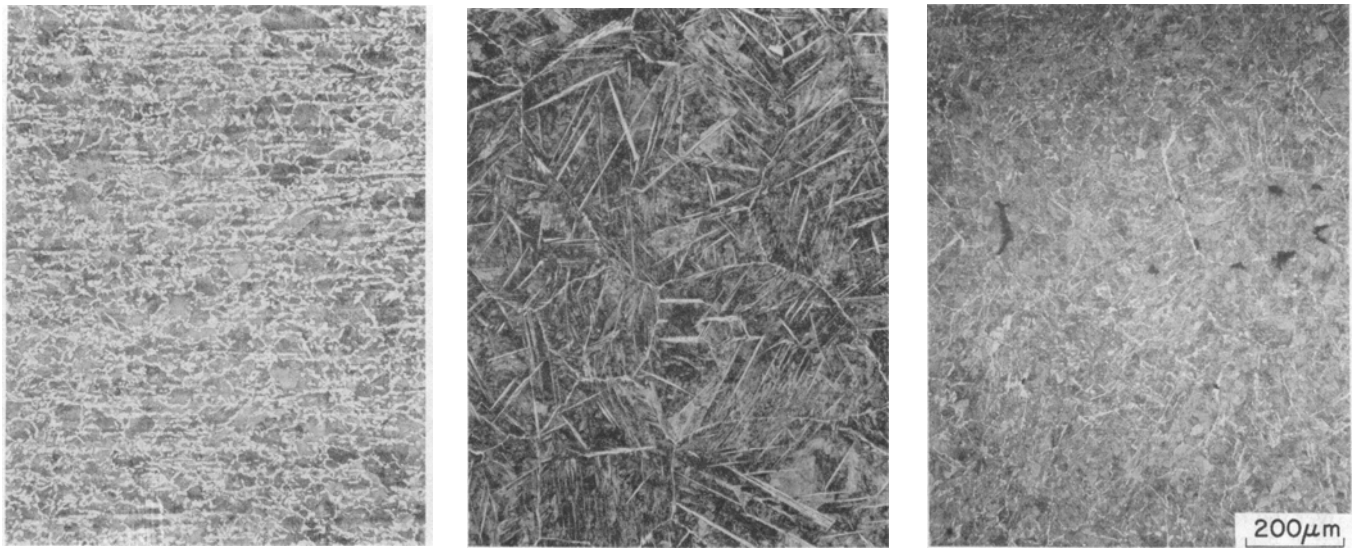

(a) (b) (c)

Fig. 27 — Three classes of microstructure produced in hypereutectoid steels after annealing 1 h in different phase regions and subsequently holding for 10 min at 600 °C before cooling. (*a*) T_A = 600 °C in pearlite + cementite region (1.89C), (*b*) T_A = 1050 °C in austenite region (1.24C), and (*c*) T_A = 1050 °C in austenite + cementite region (1.89C).

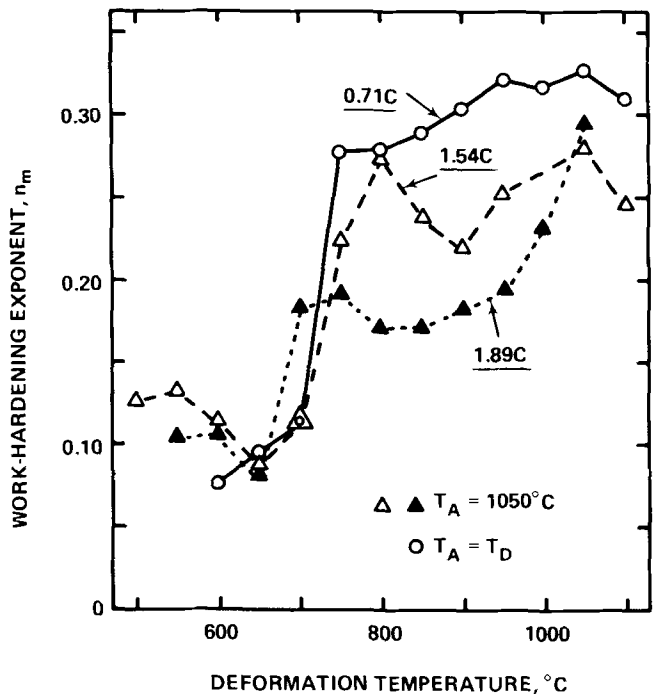

Fig. 28 — Temperature dependence of the work-hardening exponent n_m for the eutectoid steel H and the hypereutectoid steels K and JJ.

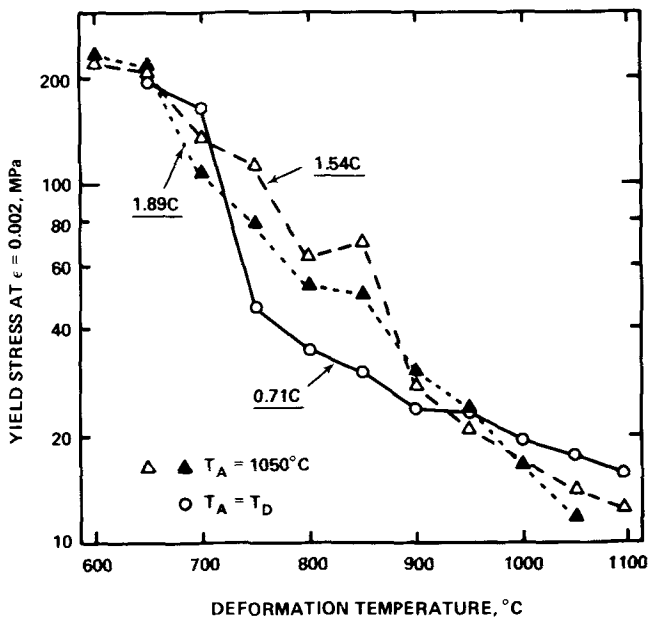

Fig. 29 — Variation of the yield stress with temperature for the eutectoid steel H and the hypereutectoid steels K and JJ.

The effect of carbon content in the austenite + cementite region is also shown by the yield stress–temperature curves in Figure 29. Over the temperature range 750 to 900 °C the cementite present in the hypereutectoid steels raises the yield stress, with the effect being greater in the 1.54C steel. Above 900 °C, if any cementite is present, it is not very effective. At 1050 °C the cementite is probably dissolved, and the solution softening of carbon in austenite is observed.[4]

IV. DISCUSSION

At elevated temperatures the most extensive phase in plain carbon steels is austenite, and the variation of the plastic flow behavior of this phase is continuous with temperature and solute content.[1-4,10] However, beyond the range of the austenite phase we find that the two-phase mixtures exhibit flow behavior which can differ sharply from that of austenite. The following discussion of these differences is arranged for low-carbon, eutectoid, medium-carbon, and hypereutectoid steels, in keeping with the interests of operators and process designers.

A. *Low-Carbon Steels*

A major feature of these steels is the substantial strength difference between austenite and ferrite. The difference is greatest at the lowest carbon contents, and it must be accounted for in any process where deformation is continuous during the phase transformation. Furthermore, the fact that low carbon steels consist mainly of ferrite below the A_3 temperature may be of some consequence. For instance, because the effect of solutes such as Mn, Si, and P is greater in ferrite than in austenite, the influence of composition is important in low-carbon steels. Secondly, the grain size of the ferrite phase is a major structural parameter which can be varied, either by thermal treatment or by alloying with elements such as phosphorus. With regard to the effect of thermal treatment, the experimental results indicate that although annealing over a broad temperature range in the austenite region can produce a large variation in austenite grain size, there is not a subsequent large variation in the ferrite grain size. This may be due to a non-linear relation between austenite and ferrite grain sizes. Consequently, varying the annealing temperature in the austenite region does not have a significant effect on the plastic flow of predominantly ferritic low-carbon steels. Why phosphorus should have such a consistent strengthening effect on the high temperature flow of ferrite is not understood.

B. *Eutectoid Steels*

Given the appropriate thermal history, eutectoid steels can consist wholely of lamellar pearlite. The high-temperature flow behavior of these steels is therefore of interest not only for its own sake, but also because lamellar pearlite is the constituent phase of medium-carbon steels. Unfortunately, there is little quantitative information in the literature regarding the plastic deformation of eutectoid steels at elevated temperatures. However, it is known that above 400 °C the cementite constituent can undergo large plastic deformation by multiple slip,[17,18] and that this high temperature plasticity is affected by the presence of Cr and Ni, but not by Mn.[19] A related finding is that the high-temperature hardness of cementite in white cast iron decreases sharply at temperatures above 500 °C.[20]

In a study of the room temperature plastic deformation of eutectoid steels,[21] it was concluded that the deformation is controlled primarily by the interlamellar spacing which in turn is determined by the cooling rate during transformation. In the case of a commercial steel, an increase in the austenitization temperature had no effect on the interlamellar spacing but did increase the pearlite colony size. However, the colony size had no significant effect on the flow stress. These observations are in agreement with a current finding that variation of T_A below 1200 °C has little effect on the flow stress at 600 °C.

The largest discontinuity in plastic flow behavior at the eutectoid temperature occurs for eutectoid steels because at this composition the relatively soft austenite transforms directly to the strong pearlite. That the strength difference is greater at the smaller strains, as shown in Figure 13, is a finding which has not been reported elsewhere in the literature. Furthermore, although not examined experimentally, it is expected that this significant difference will persist over a fairly broad range of cooling rates; the transformation to lamellar pearlite is suppressed only at rates above about 10 °C per second, and spheroidization is possible only at uneconomically slow rates of cooling. Moreover, spheroidization will probably not occur even if deformation accompanies the cooling, because the amounts of deformation which are applied during normal processing are likely to be much smaller than those used to achieve significant spheroidization.[13,14,15]

C. *Medium-Carbon Steels*

The mixture of ferrite and pearlite which exists below the eutectoid temperature in medium-carbon steels has received considerable attention in the past. Not only is the mixture of interest because of its wide use, but it is an example of a two-phase material in which the volume ratio of either phase can be changed from zero to one. Furthermore, because at room temperature the pearlite phase can be eight times stronger than the ferrite phase, some interesting property variations are possible. That considerable variation of the plastic flow behavior is also possible for this mixture at elevated temperatures has been clearly demonstrated in the present work.

Most attempts to account for the property variations of the ferrite + pearlite mixtures have been made for the room temperature behavior.[21–26] Quantitative description of the mixture's microstructure is relatively straightforward, particularly below about 0.5C where the ferrite phase is continuous. Starting with a simple law of mixtures, the solution hardening of the ferrite phase was incorporated in the models of plastic flow[21,22] along with the variation in grain size. The models have also been modified to accommodate the non-homogeneous straining of the mixture.[24]

When the modeling is eventually extended to elevated temperature behavior, it will be a test of the understanding upon which the room temperature modeling is based. In addition, at elevated temperatures the occurrence of dynamic recovery is expected to affect the strain distribution and work hardening within the mixture.

D. *Hypereutectoid Steels*

In the hypereutectoid steels the plastic flow of the pearlite plus proeutectoid cementite mixture does not show much variability with carbon content, at least not up to the level of 1.89C, partly because the total carbide content varies only by a small amount. What limits the engineering application of this strong mixture is brittle fracture, which even at elevated temperatures can occur with a reduction-in-area measure as low as 13 pct. However, if more complex processing is used to produce a fine ferrite grain structure with a fine dispersion of spheroidized cementite, high ductility is possible without a loss in strength.[8]

V. CONCLUSIONS

1. Flow behavior of plain carbon steels depends strongly on the deformation temperature, but more so above the eutectoid temperature than below.
2. In low-carbon steels the ferrite phase is considerably weaker than the austenite phase, although ferrite is more amenable to strengthening by Mn, Si, and P.

3. The existence of pearlite increases the strength below the eutectoid temperature until at the eutectoid composition the fully pearlitic structure has a higher yield stress than does the fully austenitic structure. Phosphorus strengthens lamellar pearlite as well as it does a fully ferritic structure.
4. Increasing the carbon content in hypereutectoid steels has little effect on the plastic flow behavior below the eutectoid temperature, but above that temperature cementite adds strength to the austenite matrix.

ACKNOWLEDGMENTS

The author is grateful to U.S. Steel Corporation for permission to publish this work. Discussions with L. J. Cuddy and G. R. Speich, and the technical assistance of J. J. Broderick, all of the U.S. Steel Research Laboratory, are appreciated.

REFERENCES

1. P. J. Wray and M. F. Holmes: *Metall. Trans. A*, 1975, vol. 6A, pp. 1189-96.
2. A. Palmaers: *C. R. M. Metallurgical Reports*, November 1978, no. 53, pp. 23-31.
3. T. Sakai and M. Ohashi: *Tetsu-to-Hagané*, 1981, vol. 87, pp. 2000-09.
4. P. J. Wray: *Metall. Trans. A*, 1982, vol. 13A, pp. 125-34.
5. P. J. Wray: *Met. Technol.*, 1981, vol. 8, pp. 467-71.
6. A. R. Marder: *Trans. AIME*, 1969, vol. 245, pp. 1337-45.
7. O. D. Sherby, B. Walser, C. M. Young, and E. M. Cady: *Scripta Met.*, 1976, vol. 9, pp. 569-73.
8. B. Walser and O. D. Sherby: *Metall. Trans. A*, 1979, vol. 10A, pp. 1461-71.
9. W. C. Leslie: *Metall. Trans.*, 1972, vol. 3, pp. 5-26.
10. P. J. Wray: submitted to *Metall. Trans. A*.
11. J. L. Robbins, O. C. Shepard, and O. D. Sherby: *Trans. ASM*, 1967, vol. 60, pp. 205-16.
12. E. E. Underwood: *Quantitative Stereology*, Addison-Wesley, Reading, MA, 1970, pp. 73-75.
13. E. A. Chojnowski and W. J. McG. Tegart: *Met. Sci. J.*, 1978, vol. 2, pp. 14-18.
14. H. Paqueton and A. Pineau: *J. Iron Steel Inst.*, 1971, vol. 209, pp. 991-98.
15. E. Ho and G. C. Weatherly: *J. Met. Sci.*, 1977, vol. 11, p. 141.
16. P. J. Wray: *Scripta Met.*, 1981, vol. 15, pp. 45-50.
17. A. S. Keh: *Acta Metall.*, 1963, vol. 11, pp. 1101-03.
18. A. Inoue, T. Ogura, and T. Matsumoto: *Metall. Trans. A*, 1977, vol. 8A, pp. 1689-95.
19. A. Inoue and T. Matsumoto: *Trans. Iron Steel Inst. Jpn.*, 1977, vol. 17, pp. 143-49.
20. K. B. Gove and J. A. Charles: *Met. Technol.*, 1974, vol. 1, pp. 279-83.
21. B. Karlsson and G. Linden: *Mater. Sci. Eng.*, 1975, vol. 17, pp. 153-64.
22. H. J. Kouwenhoven: *Trans. ASM*, 1969, vol. 62, pp. 437-46.
23. T. Gladman, I. D. McIvor, and F. B. Pickering: *J. Iron Steel Inst.*, 1972, vol. 192, pp. 916-30.
24. B. Karlsson and G. Linden: *Mater. Sci. Eng.*, 1975, vol. 17, pp. 209-19.
25. H. Fischmeister and B. Karlsson: *Z. Metallkd.*, 1977, vol. 68, pp. 311-27.
26. Y. Tomoto and I. Tamara: *Trans. Iron Steel Inst. Jpn.*, 1982, vol. 22, pp. 665-77.